ICES Journal of Marine Science, 61: 363–377. 2004
doi:10.1016/j.icesjms.2004.01.005

Comparing the modelled and measured target-strength variability of walleye pollock, *Theragra chalcogramma*

Elliott L. Hazen and John K. Horne

Hazen, E. L., and Horne, J. K. 2004. Comparing the modelled and measured target-strength variability of walleye pollock, *Theragra chalcogramma*. – ICES Journal of Marine Science, 61: 363–377.

Many biological and physical factors potentially affect target strength. While these sources have been identified, few studies have compared the relative effects of individual factors. Modelled and measured target strengths in non-dimensional metrics were used to compare and rank the effects of fish length, tilt, depth, and acoustic frequency on backscatter intensity. *Ex situ* measurements of target strength were used to examine the effects of tilt and depth and then compared to backscatter model predictions. Swimbladder volume reduction due to increasing pressure at depth was modelled using Boyle's law and by varying the ratio of dorsal to lateral compression. We found that length has the largest effect on the modelled and measured backscatter intensity, followed by tilt, frequency, and depth. Including tilt distributions in backscatter estimates improved the match between empirical target-strength measures and model predictions. Non-dimensional influence ratios provide insight into the sources and magnitudes of the backscatter variability.

Keywords: acoustics, backscatter, Boyle's law, depth, *ex situ* measurements, fish behaviour, frequency, model, swimbladder, target strength, tilt.

Received 22 June 2003; accepted 10 January 2004.

E. L. Hazen and J. K. Horne: University of Washington, School of Aquatic and Fishery Sciences, Seattle, WA 98195, USA. E. L. Hazen is presently at Duke University, Nicholas School of the Environment, Durham, NC 27708, USA. E-mail: ehazen@alumni.duke.edu. Correspondence to J. K. Horne: tel: +1 206 221 6890; fax: +1 206 221 6939; e-mail: jhorne@u.washington.edu

Introduction

The biology of a fish contributes to the variability in acoustic target-strength measurements (MacLennan, 1990; MacLennan and Simmonds, 1992). Tilt angle (Love, 1971; Nakken and Olsen, 1977; Blaxter and Batty, 1990), fish length (Love, 1971; Nakken and Olsen, 1977; Foote and Traynor, 1988), depth in the water (Edwards and Armstrong, 1984; Mukai and Iida, 1996; Thomas *et al.*, 2002), physiological state (Ona, 1990), and additional physical factors such as frequency (Foote, 1985; Holliday and Pieper, 1995; Horne and Jech, 1999) all influence backscatter intensity. The relative importance of these factors has been examined using predicted backscatter intensities from numerical models (Hazen and Horne, 2003).

Target-strength regression equations used in conversions of acoustic size to target size typically include length as the only independent variable (e.g. Foote and Traynor, 1988), but the inclusion of other variables may increase conversion accuracy. To accurately represent the orientations of free swimming fish populations, tilt distributions have been included in the acoustic size to fish size conversions (e.g. Foote, 1980; McClatchie *et al.*, 1996; McClatchie *et al.*, 1998). Depth has also been included as a factor in target strength-to-length conversions (Mukai and Iida, 1996) but limited research has examined how the swimbladder actually compresses under pressure (Tytler and Blaxter, 1973; Blaxter and Tytler, 1978) and the resulting effects on target strength (Ona, 1990; Gorska and Ona, 2003). At present, we do not know if the influence of any single or group of factors is limited to particular fish species or is relevant to broader categories such at physotomes and physoclists.

Target strengths can be measured or modelled but both approaches are constrained when quantifying the relative importance of biological or physical sources. *In situ* target-strength measurements incorporate ping-to-ping variability from ensonified organisms but do not permit independent measurement or the manipulation of sources that influence target strength. *Ex situ* target-strength measurements using restrained fish of known length allow target strengths to be measured while controlling tilt and depth. Backscatter models also allow the effects of length, tilt, depth, and frequency on target strength to be quantified, and to be

1054-3139/$30

examined throughout a continuous range for each variable (e.g. Horne, 2000; Hazen and Horne, 2003). Regardless of the data source, each factor's effect on target strength can be ranked. Consistency between empirically based factor rankings and those derived from backscatter models increases confidence in the results and identifies variables that warrant inclusion in acoustic size conversion models (Hazen and Horne, 2003).

In a previous study (Hazen and Horne, 2003), non-dimensional metrics were used to compare and rank the influence of fish length, tilt, depth, and acoustic frequency on target strength (Hazen and Horne, 2003). The dimensionless ratio of percent change in reduced scattering length ($RSL_{max} - RSL_{min}/RSL_{max}$) divided by percent change in a factor i ($F_{max} - F_{min}/F_{max}$) is called the influence ratio ($IR = \%\Delta RSL/\%\Delta F_i$). Influence ratio values derived from Kirchoff-ray-mode (KRM) backscatter model predictions of walleye pollock (*Theragra chalcogramma*) resulted in the ranking of factors influencing target strength as: Tilt > Frequency > Length > Depth. In this study, we compute the influence ratio values and factor rankings using *ex situ* target-strength measurements from individual fish. Rankings from the *ex situ* measurements are compared to those obtained using backscatter models to evaluate the previous model-based results and to further understand target-strength variability.

Methods

Modelling

A group of 24 walleye pollock ranging in length from 199 mm to 647 mm were used to model backscatter intensities. All fish were anesthetized in a 50-ppm bath of clove oil and ethanol (1:9 ratio) to suppress movement. Seven of the fish were raised and maintained at the Hatfield Marine Science Center in Newport, Oregon, while the remaining 17 fish were caught by trawl or hook and line at the National Marine Fisheries Service's Auke Bay Laboratory near Juneau, Alaska. While anesthetized, each fish was placed on cassettes (for fish greater than 35 cm) or reusable Flex X-ray film holders (Cone Instruments) and radiographed dorsally and laterally using a portable XTEC Laseray 90P veterinary unit. The images of fish body and swimbladder were photographed, digitized, measured, and traced. Planar data were elliptically interpolated into 1 mm thick cylinders (see Clay and Horne, 1994; Figure 2). Swimbladder lengths and surface areas were calculated from the modelled swimbladder.

Backscatter intensity was estimated using a Kirchhoff ray mode (KRM) backscattering model (Foote, 1985; Clay, 1991; Clay and Horne, 1994) that has been validated for length and tilt (Jech *et al.*, 1995; Horne *et al.*, 2000). The fish body and swimbladder are represented as gas filled and gas-filled cylinders. Backscatter intensity is calculated for each cylinder in the body and bladder and then summed coherently. When examining the effect of depth on target strength, swimbladder volume is altered according to Boyle's law. We assume equal dorsal-lateral swimbladder compression with depth unless a compression factor is stated (Table 1). A compression factor of 50% is defined as dorsal-ventral compression equal to 50% of total compression. Modelled target-strength values were compared to empirical measurements as a function of length, tilt, depth, and frequency.

Empirical backscatter measurements

After radiographing all 24 walleye pollock, the fish were ensonified using a downward-looking SIMRAD EK-60 38 kHz and 120 kHz split-beam echosounder. The echosounder was calibrated at each frequency using two spheres of known diameter and target strength (60 mm tungsten-carbide: −33.6 dB at 38 kHz; 23 mm copper: −40.4 dB at 120 kHz; Foote, 1982; Ona, 1999). Target strengths of the seven tank-reared pollock (Mean length = 44.6 cm, SD = 10.3) were measured at the Hatfield Marine Science Center in Newport, Oregon. The maximum depth at high tide was approximately 6 m and this prevented the target strength being measured as a function of depth. Tilt angles were measured over a range of −45° to 45° where 0° was horizontal. At the Alaska Fisheries Science Center's Auke Bay Laboratory, target strengths of nine (of the 17) wild-caught fish (Mean length = 29.3, SD = 4.1) were recorded while being lowered to a maximum depth of 35 m. Target strengths of 14 (of the 17) fish were also measured through a tilt range of −45° to 45°. Fish caught at Auke Bay were between 10 m and 30 m in depth and were adapted to surface pressure (e.g. visually swimming normally) prior to acoustic measurement. Handling time was limited to transferring fish from hook to tank, to an anesthetic bath, and into the monofilament sock.

For *ex situ* target-strength measurements, fish were tethered in a monofilament sock and suspended between two PVC rectangles (Figure 1). The rectangles were 1 m × 1.4 m and were connected by 3 m of monofilament line. The tethering unit was connected to two Cannon Uni-Troll downriggers (Figure 1; 1 and 2) on a disengagable axle (Figure 1; 3) so that one side of the unit can be lowered to alter fish tilt. After securing one downrigger, we lowered and raised one side of the frame in 5° tilt intervals. Lowering

Table 1. The equations used in pressure dependent isotropic and anisotropic swimbladder scaling.

$sF = (pressure_{atm})^{-1/3}$	Isotropic scaling of the swimbladder (sF)
$sFx = sF$ $sFy = 1.0 - ((1 - sF) \times 2.0 \times (1 - cf))$ $sFz = 1.0 - ((1 - sF) \times 2.0 \times (cf))$	Anisotropic scaling for lateral (sFy) and dorsal (sFz) axes using the compression factor (cf)

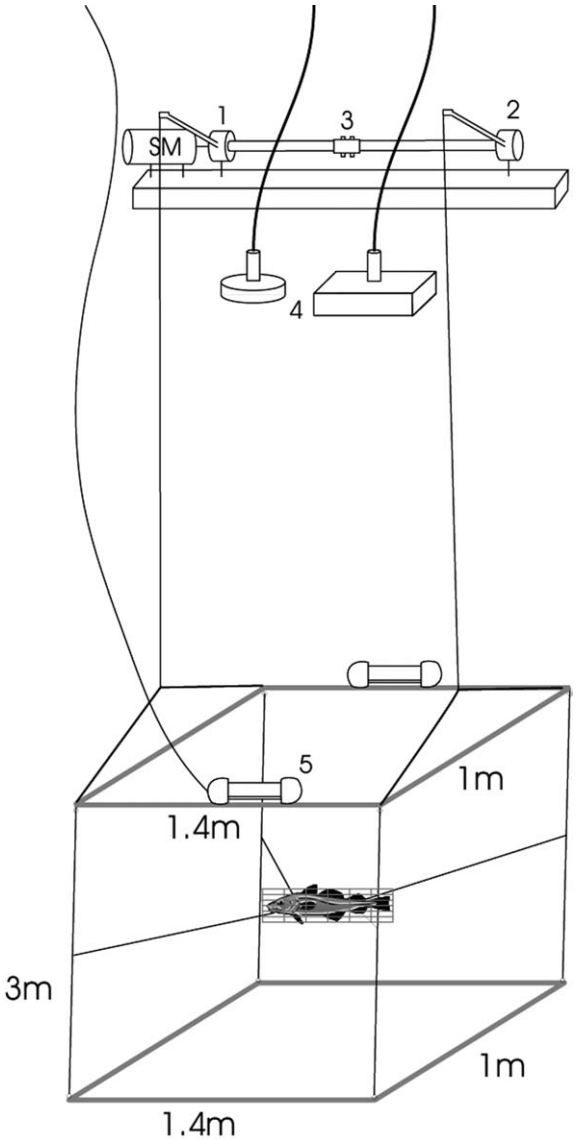

Figure 1. A schematic of the fish frame used for the controlled measurements of backscatter while manipulating tilt and depth. Two downriggers (1, 2) are connected by a disengageable axle (3) which is controlled by the stepper motor (SM). A 38 kHz and 120 kHz SIMRAD EK-60 echosounder (4) measures echo amplitude. Tilt was measured using a clinometer (5) mounted on the top frame. The fish is held within the frame by four monofilament lines connected to a sock.

the line on both downriggers increased the depth of the fish. A stepper motor (Figure 1; SM) was programmed to control the timing and the amount of line lowered through a depth range of 2−35 m. An Applied Geomechanics biaxial clinometer (Figure 1; 5) was placed on the upper frame to measure the tilt of the fish. An empty housing was mounted on the frame across from the clinometer to balance the frame. Tilt values were recorded in synchrony with the transmitted pulses from the echosounder. *In situ* target strengths of fish swimming near the tilt frame were also collected during *ex situ* measurements.

All acoustic data processing used Sonardata's Echoview software to extract single echoes (i.e. targets) between the lower and upper frame and from free-swimming fish below the frame. Single-target acceptance parameters were set at: −70 dB TS threshold, 6.0 dB pulse length detection level, 0.8 and 1.5 for minimum and maximum normalized pulse length, 10 dB maximum beam compensation, and 3° maximum standard deviation of minor and major axis angles. When more than one target was present in the beam between the two frames, target-strength measurements were excluded from the data set.

Analysis

Measured target strengths at dorsal aspect (i.e. horizontal fish position) were converted to non-dimensional, reduced scattering lengths (RSLs) and averaged across all measurements within 1 m depth bins. Angle dependent target strengths (i.e. measured while varying tilt within the −45° to 45° arc) were averaged across measurements within 5° tilt-bins for each fish.

Measured target strengths were compared to KRM model predictions and literature values at 38 kHz and 120 kHz. Scaled fish lengths (150−650 mm) are calculated by scaling each fish proportionately in all dimensions. Scaling fish length produces a continuous range of lengths enabling comparison over any interval range. The KRM model-predicted target strengths for all fish were averaged across the scaled length range in 1 m bins. Backscatter was also modelled for each fish at its original length and 90° tilt. Predicted and measured backscatter intensities at length were also compared to Foote and Traynor's (1988) empirically derived target strength−length equation at 38 kHz:

$$TS = 20\log(L_{cm}) - 66. \quad (1)$$

Tilt-averaged, target-strength distributions were derived for each fish using a simulated tilt distribution and the corresponding modelled or measured target strengths. Simulated tilt distributions were calculated for each fish by randomly selecting 1000 angles from a normal distribution with a mean of 0° and a standard deviation of 15°. These parameters are consistent with those observed for walleye pollock and other gadoid fish species (Huse and Ona, 1996; McClatchie *et al.*, 1996; Horne, 2003). Once a tilt angle was chosen, the corresponding target strength was extracted from the plotted target strength versus tilt angle curve for each fish. Target strengths incorporating a normal tilt distribution and target strengths at dorsal incidence were regressed against log(length), log(swimbladder length), and log(swimbladder area). The regression fit to the data was quantified using Pearson product moment

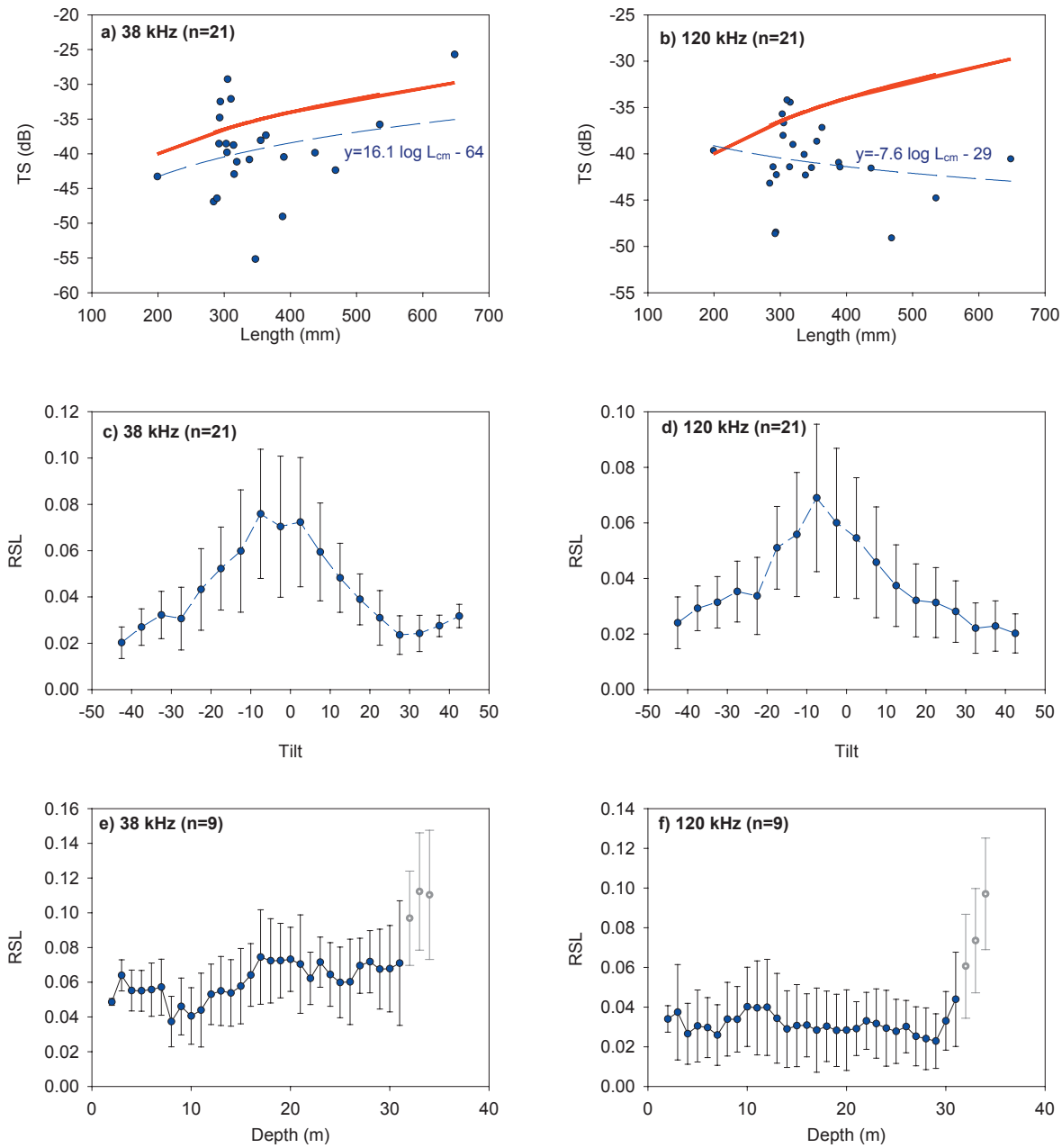

Figure 2. Measured target strengths plotted as a function of (a) length at 90° tilt at 38 kHz (dashed), (b) length at 90° tilt at 120 kHz (dashed), (c) tilt averaged in 5° bins at 38 kHz, (d) tilt averaged in 5° bins at 120 kHz, (e) depth averaged in 1 m bins at 38 kHz, (f) depth averaged in 1 m bins at 120 kHz. Grey points have sample sizes of two fish or less and were not included in the analyses. Equation (1) ($TS = 20 \log L_{cm} - 66$) is included as a continuous line in plots of TS at length at both frequencies for reference.

correlation coefficients (r^2) calculated between regression predicted, and measured or modelled target strengths.

Target strengths at depth were examined by using Boyle's law to model swimbladder compression at depth, using the KRM model to compute acoustic backscatter, and then comparing modelled to empirically measured TS values using Pearson product moment correlation coefficients (r^2). The compression factor (i.e. the ratio of dorsal/ventral compression) of the swimbladder was varied from 20% to 90% in 10% increments, while maintaining a gas volume consistent with Boyle's law (cf. Table 1). The mean and standard deviation of the measured target strength–tilt curve was used to parameterize a normal distribution of target strengths at tilt (Foote, 1980). Modelled and

measured target strength–tilt curves were tested for deviation from the calculated normal distribution of target strengths at tilt using a chi-squared test.

Because each biological or physical factor is measured using unique units (tilt, degrees; depth, metres; length, millimetres; frequency, kilohertz), non-dimensional metrics were used to compare and quantify the relative influence of each factor on backscatter intensity (Hazen and Horne, 2003). Maximum influence ratios (MIRs) were calculated using the ratio of the maximum percent change in RSL for each factor to the equivalent percent change in the factor. MIR values were then ranked to determine the relative maximum influence of each factor on target strength.

Contour plots were used to compare influence ratios at specific values within intervals, and to graphically contrast each factor's relative influence on backscatter intensity. Each influence ratio is calculated from the smallest value within a factor's range at an interval size of one, through the maximum value. The process is repeated, increasing the interval size until the interval is equal to the entire range for that factor. In the presentation of results, the interval size of factor A is plotted on the x-axis (length for this study) and the interval size of factor B (tilt, depth, and frequency) is plotted on the y-axis. Contoured values are equal to the influence ratio for factor B divided by the influence ratio for factor A (i.e. IR_B/IR_A). If this comparison ratio is greater than one, factor B has a greater influence on TS at the interval sizes specified. If less than one, factor A has a greater influence on TS. If the ratio value is approximately one, both factors have equal influence on target strength. Both maximum influence ratios and contours are used to rank the relative influence of each factor.

Results

Each factor's effect on backscatter intensity was examined individually before being compared to the influence of other factors. Because free-swimming fish were ensonified below the tilt frame in Auke Bay, *in situ* target strengths could also be extracted from the acoustic data. The mean *in situ* target strength of 850 tracked fish that passed through the 38 kHz beam was −38.7 dB. Using Equation (1) to convert mean TS to length, the predicted length of these fish was 232 mm, with a standard deviation of 130 mm. The 17 fish caught using hook and line from the wharf adjacent to the tilt frame had a similar mean length of 297 mm, with a standard deviation of 43 mm.

TS values were plotted on the y-axis with length, tilt, and depth on the x-axis at 38 kHz and 120 kHz for each fish. Target strengths were converted to linear units and averaged by tilt and depth bin for all fish (Figure 2). The slope of the log-linear regression between length and dorsal-aspect TS was positive at 38 kHz but negative at 120 kHz (Figure 2a, b). The relationship between tilt and average RSL was normally distributed [$N_{38}(0.043,0.018)$; $N_{120}(0.038,0.015)$] at both frequencies ($\chi^2_{38} = 0.030$, $\chi^2_{120} = 0.023$, $p = 1$, $df = 20$; Figure 2c, d). Depth was not related to RSL at 38 kHz or at 120 kHz ($p > 0.05$), and was highly variable (Figure 2e, f). Average RSL increased below 31 m at both frequencies but the sample size was restricted to two fish at 32 m and one fish deeper than 32 m. These two fish were average in size (292 mm and 293 mm) but had larger average target strengths than the other seven fish. The mean *ex situ* measured target strengths at 90° incidence was almost 3 dB higher than the mean *in situ* extracted target strengths (*in situ* mean TS = −38.7 dB, *ex situ* mean TS = −35.3 dB).

A log-linear regression of fish length and *ex situ* measured target strength was parameterized at 38 kHz and 120 kHz using two models ($TS = \beta_1 \times \log(\text{length}) + \beta_0$, $TS = 20 \times \log(\text{length}) + \beta_0$; Table 2). The regression of measured target strength on length had slopes and intercepts closer to those in Equation (1) when a normal tilt distribution (Mean tilt angle = 0°, SD = 15°; Figure 3) was included in the target-strength calculations than when target-strength values were modelled and measured at 90° (Table 2). The 120-kHz measured target strength–length regression calculated at 90° had a slope and intercept not significantly different from zero ($\alpha = 0.05$; $p(\beta_1) = 0.36$, $p(\beta_0) = 0.31$). Slopes and intercepts from regressions of measured and modelled target strengths and length (Figure 3) were significantly different from zero at both frequencies when incorporating a normal tilt distribution ($p < 0.05$). Equation (1) (Foote and Traynor, 1988) is shown for reference at both frequencies.

When tilt-averaged modelled target strengths were compared to measured target strengths for each fish, walleye pollock number 74 at 120 kHz showed the highest correlation ($r^2 = 0.92$, Figure 4a). Walleye pollock 57 showed poor correlation between modelled and measured target strengths as a function of tilt ($r^2 = 0.27$, Figure 4b). The same plot averaged across all fish also shows a strong correlation between modelled and measured target strengths at 38 kHz ($r^2 = 0.68$) and 120 kHz ($r^2 = 0.80$,

Table 2. Tilt distributed (mean = 0°, SD = 15°) and horizontal TS–length logarithmic regressions ($\beta_1 \times \log L_{cm} - \beta_0$) at 38 kHz and 120 kHz for measured and KRM model predicted target strengths.

		120 kHz			38 kHz		
		β_1	B_0	r^2	β_1	B_0	r^2
Normal	Modelled	20.8	−70	0.88	17.4	−63	0.78
		20	−69	0.88	20	−67	0.77
	Measured	9.7	−52	0.16	22	−69	0.18
		20	−68	0	20	−66	0.18
Horizontal	Modelled	19.2	−85	0.33	7.1	−53	0.081
		20	−88	0.33	20	−86	0
	Measured	−7.5	−22	0.038	16.1	−80	0.069
		20	−92	0	20	−86	0

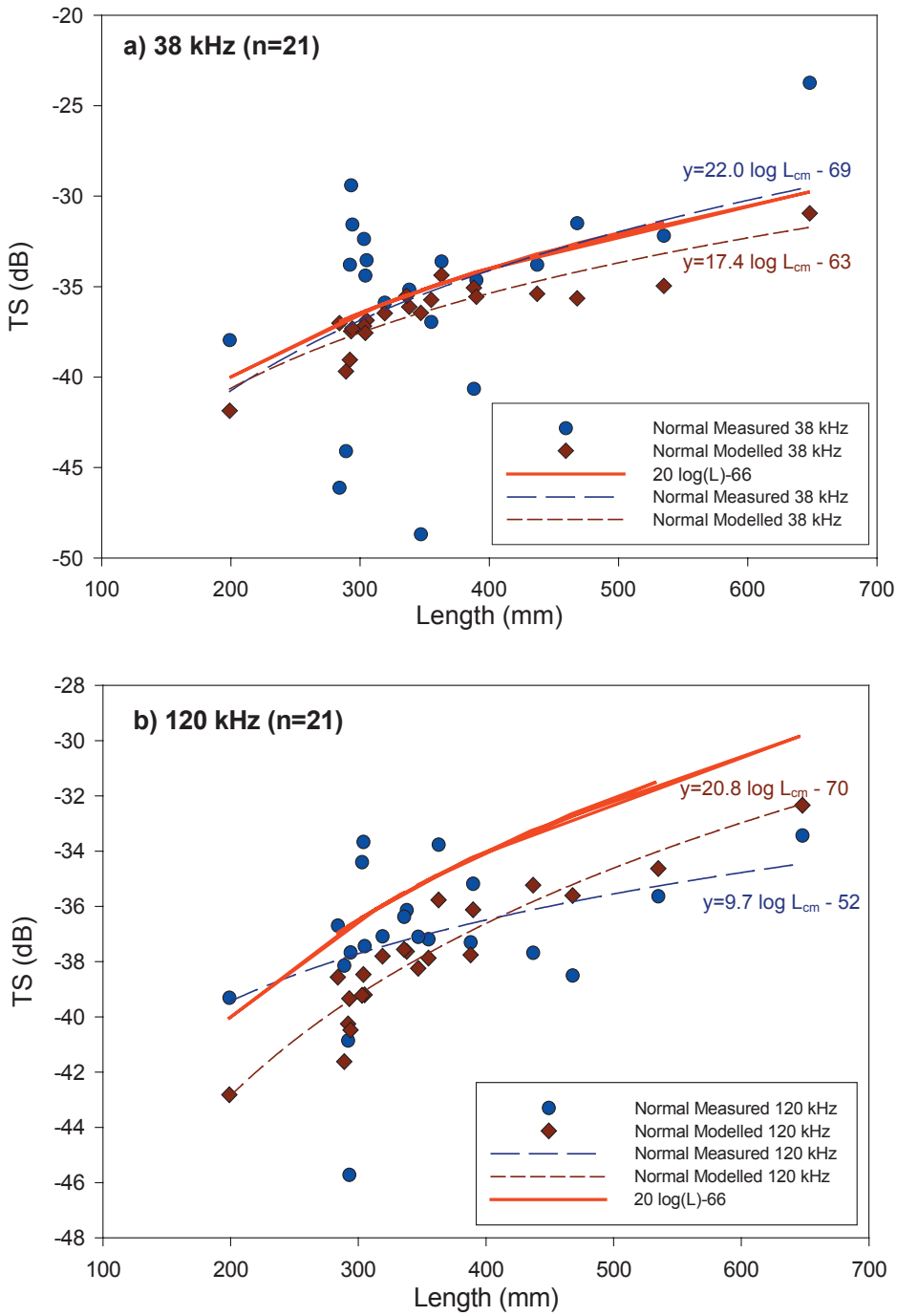

Figure 3. Modelled and measured target strengths plotted as a function of fish length assuming a normal tilt distribution (mean = 0, SD = 15) for 21 fish at (a) 38 kHz and (b) 120 kHz.

Figure 5). Swimbladder length, swimbladder dorsal surface area of each fish, and averaged depths were all correlated with measured target strengths at dorsal aspect (all $r^2 < 0.4$). Target strength at depth modelled with a compression factor of 90% was the closest match to empirical data at 120 kHz, with target strengths increasing after 8-m depth (Figure 6).

Maximum influence ratios compare each factor's maximum influence using modelled and measured data. MIR values were calculated separately for Newport tank-reared

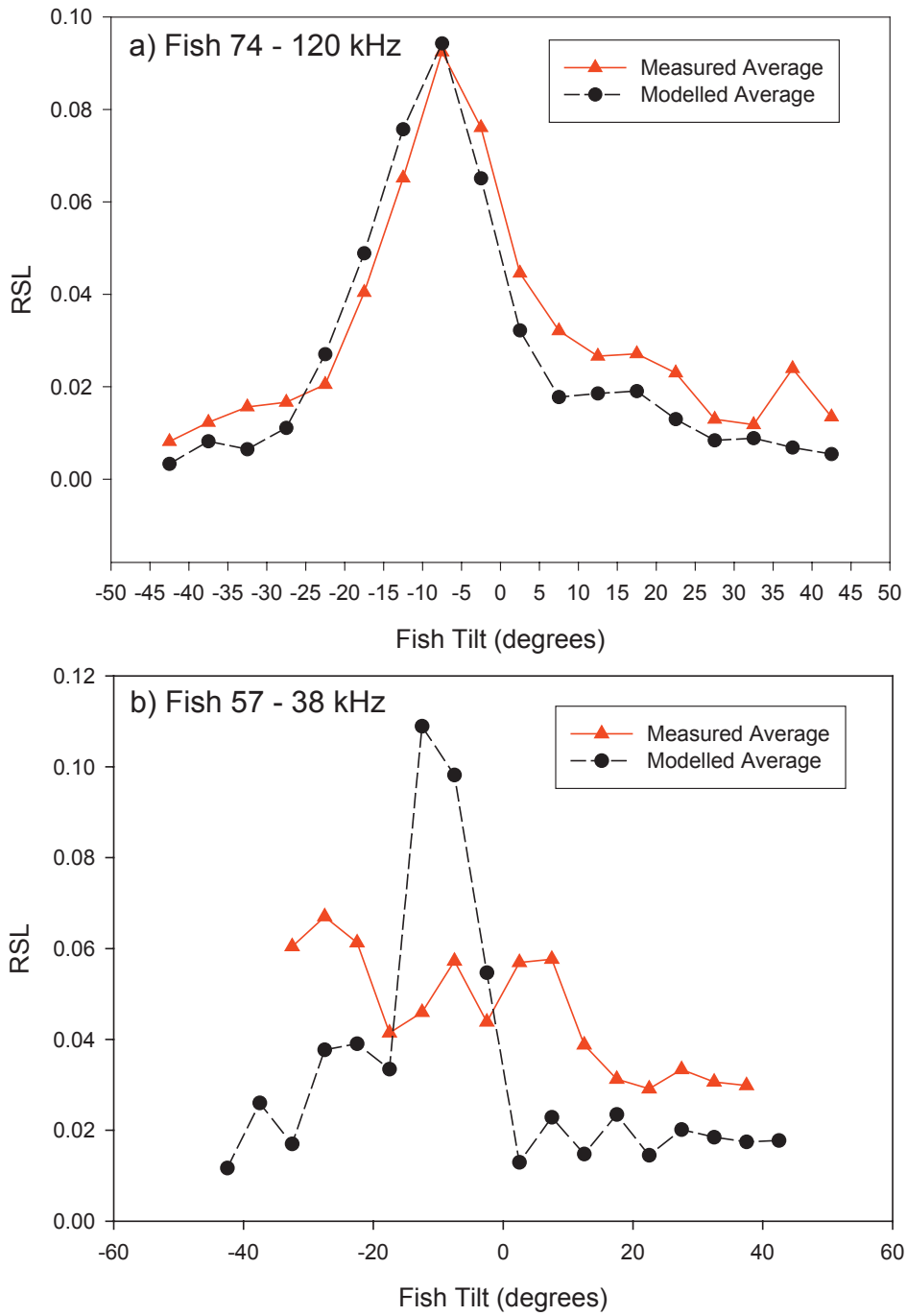

Figure 4. (a) A plot of modelled RSL and measured RSL for walleye pollock number 74 at 120 kHz. Modelled and measured backscatter data were highly correlated ($r^2 = 0.92$). (b) A plot of modelled RSL and measured RSL for walleye pollock number 57 at 38 kHz. The correlation between the modelled and measured backscatter data was poor ($r^2 = 0.27$).

fish and Auke Bay wild-caught fish at 38 kHz and 120 kHz. There was no difference in the rankings of influence ratios between frequencies, between tank-reared and wild fish, or between modelled and measured MIR values. Among modelled MIR values, length had the greatest influence on backscatter: Length > Tilt > Frequency > Depth (Table 3). As a slight contrast, fish depth above 30 m had a greater influence on target strength than frequency among *ex situ*

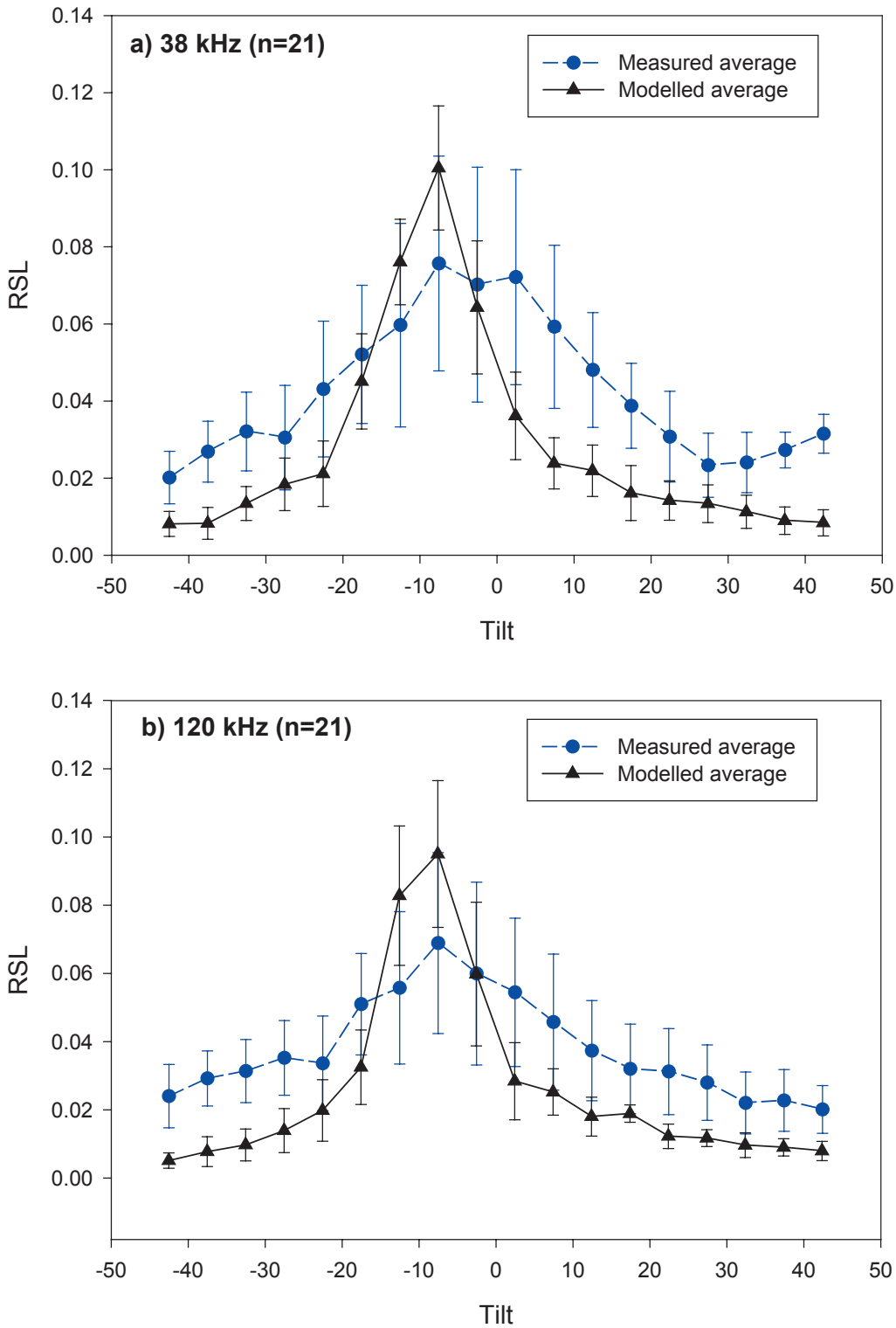

Figure 5. The modelled and measured reduced scattering length (RSL) plotted as a function of fish tilt for (a) 38 kHz and (b) 120 kHz.

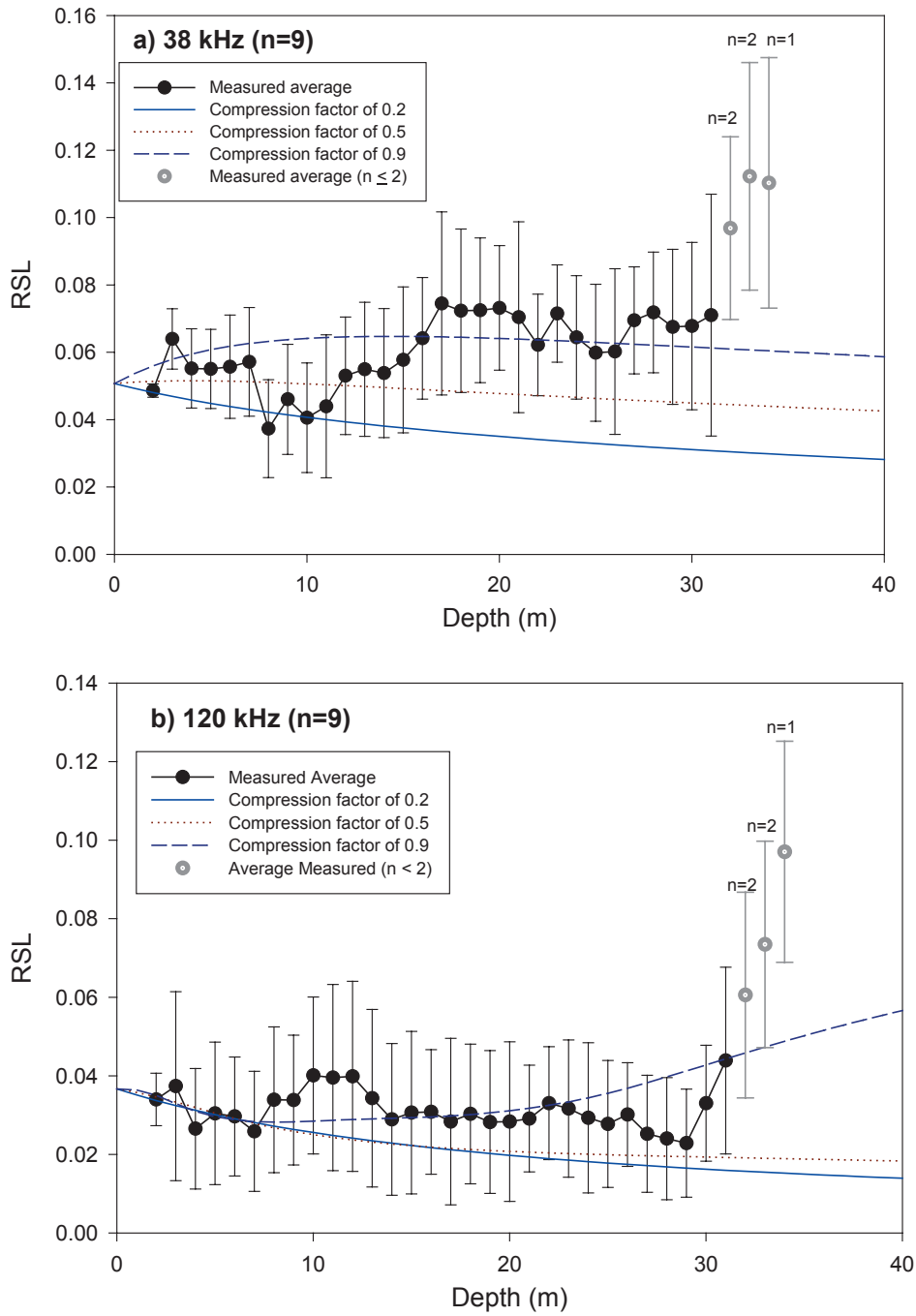

Figure 6. The modelled and measured reduced scattering length (RSL) regressed against depth at 38 kHz and 120 kHz. Modelled values assume compression factors of 0.2, 0.5, and 0.9 for the proportion of compression that occurred in the dorsal-ventral axis. At depths greater than 31 m, the sample size decreased to two fish.

measured target strengths in Auke Bay (Table 4): Length > Tilt > Depth > Frequency.

To allow comparison ratios to be calculated over continuous intervals, backscatter intensity was calculated from individual fish that were proportionately scaled between 150 mm and 650 mm in length at 1 mm increments. The plot of scaled length as a function of frequency shows that most comparison ratios are greater than one (plotted as curves; Figure 7), indicating that frequency has a greater effect on modelled TS than scaled length at most

Table 3. The maximum influence ratios (MIRs) calculated from modelled TS for length, tilt, frequency, and depth. MIRs for modelled length are calculated between two individuals to incorporate morphological variability.

Modelled	Fi	Range	ΔFi	ΔRSL	%ΔFi	%ΔRSL	MIR
Newport tank	Length	347–648 mm	121 mm	0.055	0.26	0.67	**2.58**
	Tilt	45°–135°	35°	0.095	0.74	0.93	**1.27**
	Frequency	38 and 120 kHz	82 kHz	0.014	0.68	0.23	**0.341**
Auke Bay Wild	Length	199–390 mm	44 mm	0.085	0.13	0.77	**5.88**
	Tilt	45°–135°	35°	0.087	0.74	0.95	**1.29**
	Frequency	38 and 120 kHz	82 kHz	0.015	0.68	0.20	**0.299**
	Depth	0–30 m	30 m	0.017	0.88	0.15	**0.168**

interval sizes. Most ratio values derived from empirical measures (plotted as points) are less than one, indicating that changes in TS due to frequency are less influential than changes due to fish length. Modelled effects of tilt have a greater influence on TS than the effects of scaled length on TS, except at extreme tilt angles (Figure 8). At equal interval sizes, the comparison ratios of tilt and fish length indicate that length has a greater effect on measured TS than tilt. However, the results among pairs of fish varied. One pair of fish that differed by over 200 mm in length had similar TSs and corresponding comparison ratio values of 8.0 at "large" length intervals. A few pairs of fish that differed by less than 10 mm in length had very different TSs and corresponding comparison ratio values of 0.2 at "small" length intervals. The switching of comparison ratio values above and below one among fish pairs suggests that tilt and length can have similar influences on measured target-strength values. Comparison values greater than one at equal interval sizes indicate that depth has a greater influence on modelled TS compared to that of scaled length (Figure 9). All comparison ratio values were less than one when comparing the influence of depth to fish length on measured TS. Modelled and measured contoured results at both frequencies show similar results that differ only in magnitude.

Discussion

Maximum influence ratios and comparison ratio plots provide categorical and graphical rankings of each factor's influence on TS over a range of interval sizes. Because relative rankings of depth and frequency effects on TS were similar, the hierarchical ranking of:

$$\text{Length} > \text{Tilt} \gg \text{Depth} \approx \text{Frequency}$$

is most credible. Tilt and length have similar comparison ratio values and maximum influence ratio values close to 2. Frequency and depth have similar MIR values (≈ 0.4) and therefore less influence on target strength than tilt and length. The relative influences of length, tilt, depth, and frequency on walleye pollock target strength should be common in other physoclist species (cf. Midttun, 1984; Foote, 1987). It is worth noting that rankings could change among populations and over time but we attempt to minimize local variations by calculating maximum potential differences in ratio values and by using equal intervals to expose changes in influence through factor ranges. As a natural extension of the technique, comparison of ratio values among species could be used to index similarities or differences in the relative influence among biological factors on target strength.

We attribute the difference in rankings between comparison ratio values calculated using modelled (i.e. scaled) fish lengths (Hazen and Horne, 2003) and those derived using measured fish lengths to intra-specific variation in fish morphology. This point is graphically illustrated by the 15 dB range in predicted and measured target strengths among a group of 21 fish, 300 mm long (Figure 3). KRM model predictions and subsequent ratio values for any two individual fish are affected by

Table 4. The maximum influence ratios (MIRs) calculated from measured TS for length, tilt, frequency, and depth.

Measured	Fi	Range	ΔFi	ΔRSL	%ΔFi	%ΔRSL	MIR
Newport tank	Length	347–648 mm	147 mm	0.034	0.28	0.56	**2.05**
	Tilt	45°–135°	50°	0.036	0.38	0.66	**1.75**
	Frequency	38 and 120 kHz	82 kHz	0.0085	0.68	0.18	**0.268**
Auke Bay Wild	Length	199–390 mm	93 mm	0.091	0.32	0.76	**2.40**
	Tilt	45°–135°	45°	0.051	0.34	0.72	**2.11**
	Frequency	38 and 120 kHz	82 kHz	0.019	0.68	0.24	**0.31**
	Depth	0–30 m	26 m	0.029	0.90	0.55	**0.619**

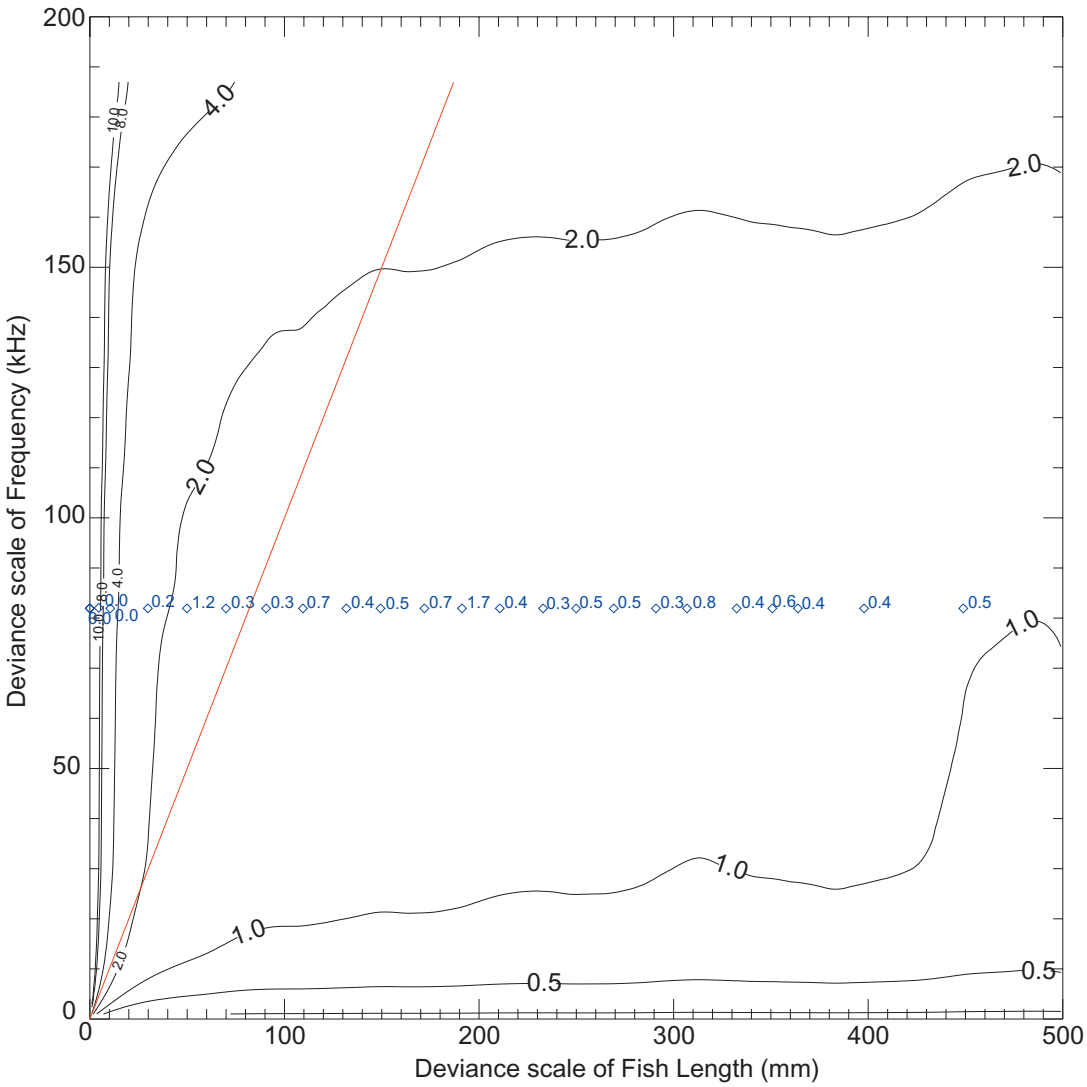

Figure 7. A contour plot of comparison ratios for the effects of frequency (12−200 kHz) on backscatter intensity divided by the effect of scaled length (150−650 mm). The x- and y-axes are the interval sizes for each factor. The unlabelled line identifies equal interval sizes. Measured comparison ratios are overlaid as grey points where length includes morphological variability while modelled length is scaled.

differences in shape as well as fish size. Yet despite anatomical differences among fish, the target strength to length regression for this walleye pollock group matches target strengths predicted in Equation (1) (Table 2). MIR values from our previous study were calculated using a group of fish scaled across lengths rather than actual length differences among fish. Because every fish within a group is scaled to each length, differences in TS calculated among scaled lengths is attributed primarily to differences in length rather than differences in shape. In this study, all measured and modelled target strengths and the resulting MIRs were calculated using individual fish lengths rather than scaled fish lengths. Differences in influence ratios calculated using fish lengths from those using scaled fish lengths could be used to understand the non-linear effects of morphology on target strength.

Consistent relationships between individual variables and modelled or measured target strengths were not observed in this study. A relationship between dorsal swimbladder area and target strength may be expected as most acoustic fish surveys use geometric scattering frequencies. No strong relationship ($r^2 < 0.4$) was found between swimbladder surface area or swimbladder length and measured target strength, indicating that the relationship is more complex than swimbladder shape alone for walleye pollock. In contrast, Jørgensen (2003) observed that the relationship between swimbladder length and target strength was stronger than that between fish length and target strength among capelin (*Mallotus villosus*).

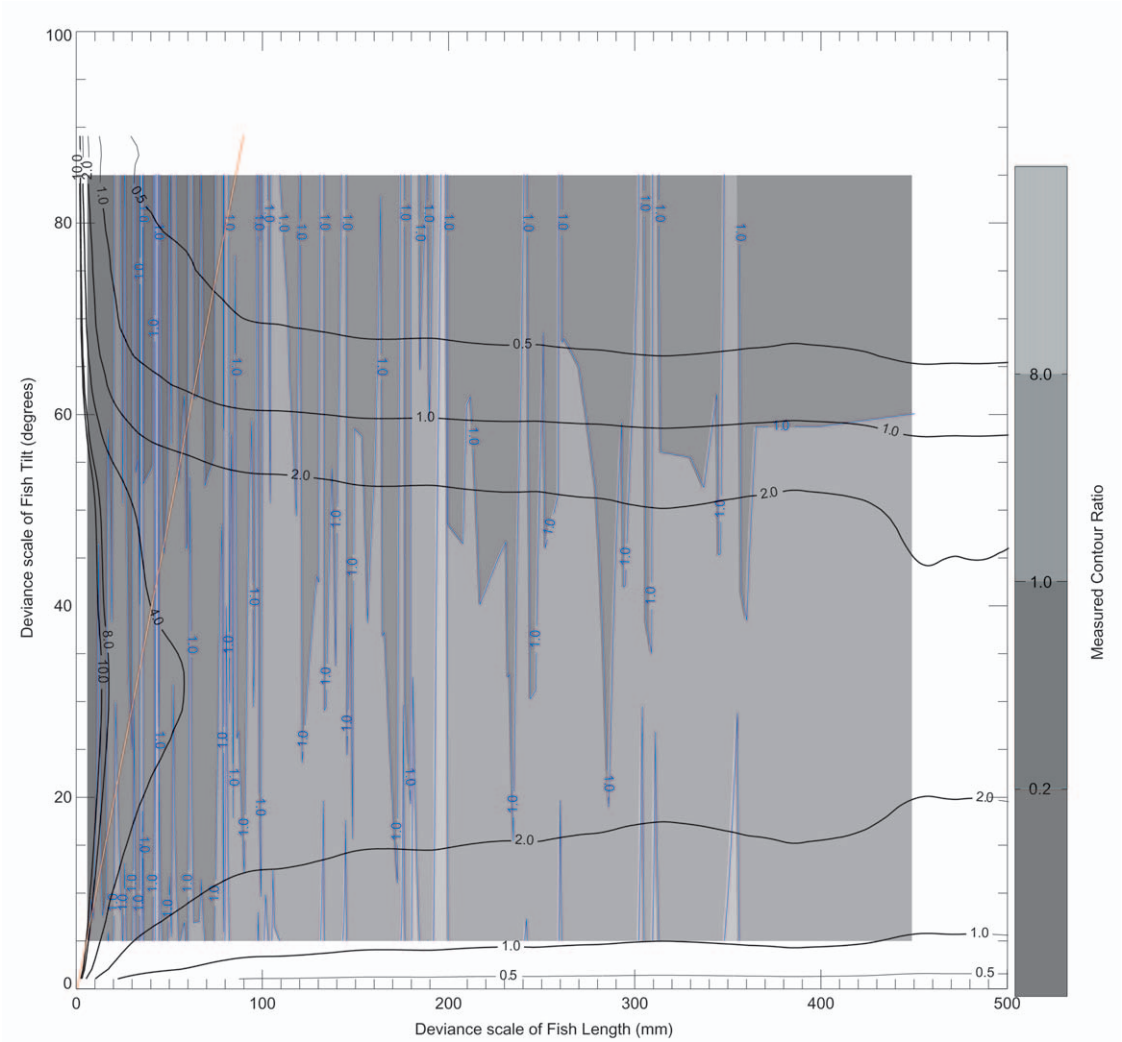

Figure 8. A contour plot of comparison ratios $[(\%\Delta RSL/\%\Delta F_A)/(\%\Delta RSL/\%\Delta F_B)]$ for the effects of tilt (45°−135°) on backscatter intensity divided by the effects of scaled length (150−650 mm) at 120 kHz. The x- and y-axes are the interval sizes for each factor. The unlabelled line identifies equal interval sizes. Measured comparison ratios are overlaid as a filled contour with the labelled lines drawn at values of 1.0. Measured length includes morphological variability among fish while modelled lengths scale each fish through the entire length range.

Depth was also not a good predictor of target strength in this study. Target strength has been shown to decrease with depth for gadids (Edwards and Armstrong, 1984; Ona, 1990), salmonids (Mukai and Iida, 1996), and herring (Huse and Korneliussen, 2000; Thomas *et al.*, 2002) but we did not observe a continuous decrease in target strength with any instantaneous change in depth. The maximum change in measured target strength observed for fish in this study, 4 dB over 30 m at 120 kHz (Figure 2), is consistent with reductions in target strength predicted using swimbladder compression (cf. Ona, 1990; Mukai and Iida, 1996; Thomas *et al.*, 2002). Additional studies on fish behaviour, pressure effects on the swimbladder (instantaneous and changes over time), and resulting target strength are needed. The challenge when collecting empirical measures is separating the effects of depth from the effects of behaviour during *in situ* or caged measurements (e.g. Huse and Korneliussen, 2000; Orlowski, 2001).

Fish swimbladders are not expected to compress isometrically due to physical constraints by the pleural ribs and spinal column (Foote, 1985; Ona, 1990). The 90% dorso-ventral compression ratio used in KRM modelling provided the best match to empirical data while varying depth and predicted an increase in target strength at 120 kHz. Gorska and Ona (2003) observed that the match between modelled target strengths and measured values was best when the compression of dorsal swimbladder area was minimized, suggesting that most of the swimbladder contraction occurs in the dorso-ventral plane.

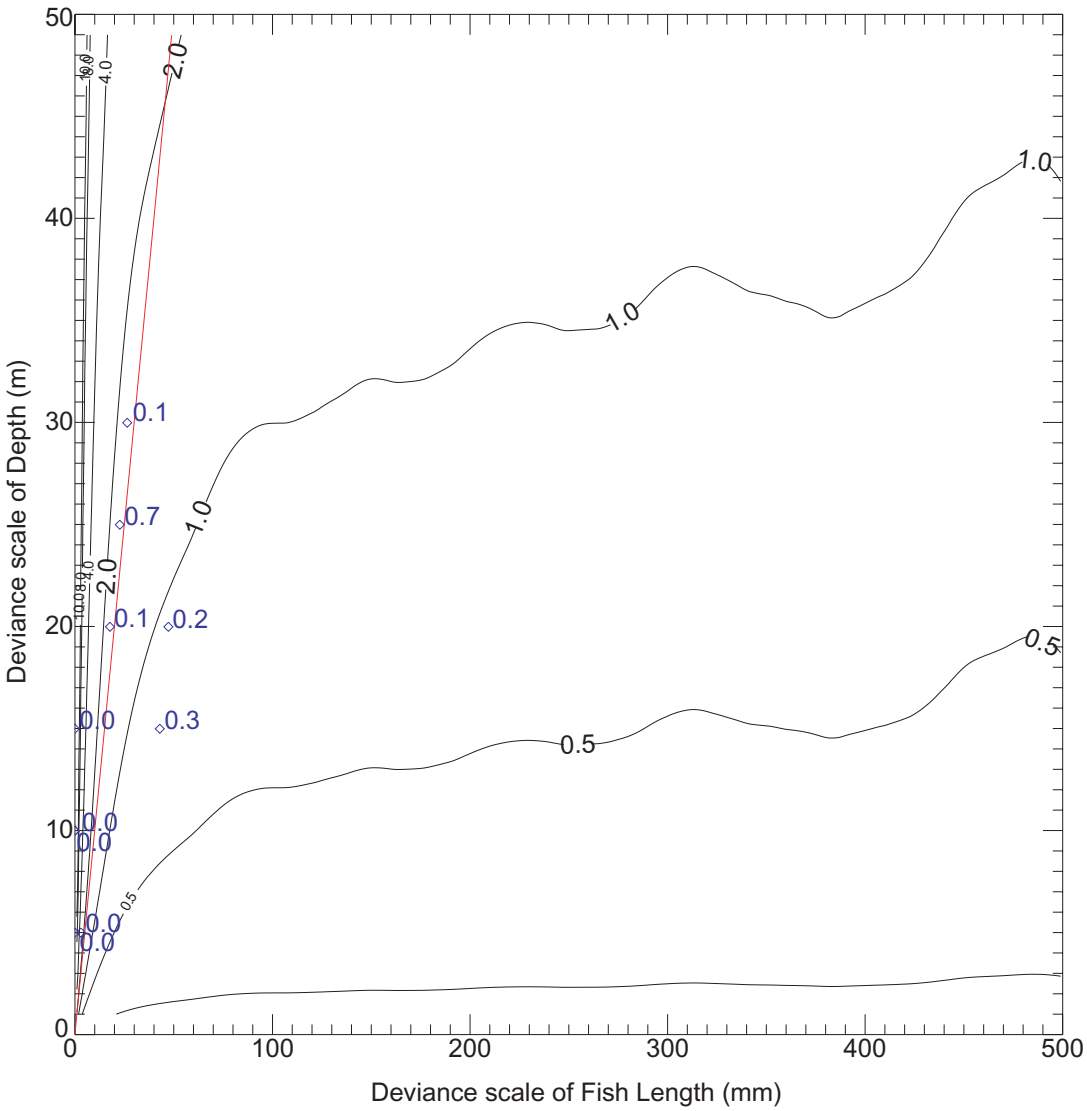

Figure 9. Comparison ratios for the effects of depth (0−50 m) on backscatter amplitude divided by the effects of scaled length (150−650 mm) at 120 kHz. The x- and y-axes are the interval sizes for each factor. The unlabelled line identifies equal interval sizes. Measured comparison ratios are overlaid as open diamonds. Measured length includes morphological variability among fish while modelled lengths scale each fish through the entire length range.

Target strengths were consistently larger near dorsal incidence and smaller at extreme tilt angles. Tilt-dependent modelled and measured target-strength values were similar to previous tilt and target-strength studies of walleye pollock (Sawada *et al.*, 1999) and Atlantic cod (Foote, 1980). We found a 13 dB maximum target-strength change over the 90° tilt range (−45° to 45°). The maximum observed target strength occurred at a 7.5° head down orientation (Figure 2). Tilt distributions of single or groups of fish are not static and can change based on time of day (Huse and Ona, 1996; Orlowski, 2001), avoidance of vessels (Vabø *et al.*, 2002), or predators (Nøttestad, 1998). It is important to sample at a rate that will record changes in tilt (Hazen and Horne, 2003). To prevent tilt angles from biasing regression predicted target strengths, tilt distributions should be measured and parameterized in acoustic size to fish length conversions (MacLennan *et al.*, 1990; McClatchie *et al.*, 1998; Huse and Korneliussen, 2000).

Current acoustic size to fish length conversions implicitly average effects of tilt on target strength. We found that target strengths that incorporated a normal tilt distribution (Mean tilt = 0°; SD = 15°) matched previous TS−length regressions for walleye pollock (Foote and Traynor, 1988; Table 3) better than dorsal incidence measures alone.

A TS–length regression that incorporates normal tilt distributions matched the slope and intercept at 38 kHz (Equation (1)) and differed slightly at 120 kHz (Table 2):

$$TS = 20\log L_{cm} - 68.5 \quad (2)$$

The agreement between modelled, measured, and regression predicted target strengths is reassuring.

Non-dimensional influence ratios provide insight to sources and magnitudes of backscatter variability. The relative ranking of influence ratios can be used to identify factors that should be explicitly included in target-strength conversions. The factor rankings suggested by this study differ from those based entirely on KRM backscatter model predictions (Hazen and Horne, 2003). Even though differences existed between measured and modelled target strengths, both resulting factor rankings suggest that tilt should be included in target-strength estimates. Target tracking (e.g. Ehrenberg and Torkelson, 1996; Huse and Ona, 1996; Ona, 2001) and observational measurements of tilt angle distributions provide two methods of obtaining realistic tilt-angle frequency distributions for inclusion in conversions of acoustic size to fish length (Foote, 1980; Foote and Ona, 1987; MacLennan *et al.*, 1990). Large target-strength sample sizes will ensure that the stochastic nature of target-strength variability is included in acoustic size estimates (e.g. Dawson and Karp, 1990; Horne *et al.*, 2000). A final requirement needed to validate the utility of this method is a comparison of factor rankings between physoclist and physostome fish species.

Acknowledgements

This study was funded by the US Office of Naval Research (N00014-00-1-0180) and the ARCS foundation of Seattle. Thanks go to the staff of the Fisheries Acoustics Research Laboratory for all their help and especially Jason Sweet for assistance with data collection and Rick Towler for programming support. We also thank Al Stoner, Michael Davis, Erick Sturm, and Michele Ottmar from the Alaska Fishery Science Center in Newport, OR, and Mike Sigler and Johanna J. Vollenweider from the Alaska Fishery Science Center in Auke Bay, AK, for their help with access to fish and to laboratory space for the radiographs and measurements.

References

Blaxter, J. H. S., and Batty, R. S. 1990. Swimbladder "behaviour" and target strength. Rapports et Procès-Verbaux des Réunions Conseil International pour l'Exploration de la Mer, 189: 233–244.

Blaxter, J. H. S., and Tytler, P. 1978. Physiology and Function of the Swimbladder. Advances in Comparative Physiology and Biochemistry, vol. 7. Academic Press, New York.

Clay, C. S. 1991. Low-resolution acoustic scattering models: fluid-filled cylinders and fish with swimbladders. Journal of the Acoustical Society of America, 89: 2168–2179.

Clay, C. S., and Horne, J. K. 1994. Acoustic models of fish: the Atlantic cod (*Gadus morhua*). Journal of the Acoustical Society of America, 96: 1661–1668.

Dawson, J. J., and Karp, W. A. 1990. *In situ* measures of target-strength variability of individual fish. Rapports et Proces-Verbaux des Reunions Conseil International pour l'Exploration de la Mer, 189: 264–273.

Edwards, J. L., and Armstrong, E. 1984. Target-strength experiments on caged fish. Scottish Fisheries Bulletin, 48: 12–20.

Ehrenberg, J. E., and Torkelson, T. C. 1996. Application of dual-beam and split-beam target tracking in fisheries acoustics. ICES Journal of Marine Science, 53: 329–334.

Foote, K. G. 1980. Effect of fish behaviour on echo energy: the need for measurement of orientation distributions. Journal de Conseil International pour Exploration de la Mer, 39(2): 193–201.

Foote, K. G. 1982. Optimizing copper spheres for precision calibration of hydroacoustic equipment. Journal of the Acoustical Society of America, 71(3): 742–747.

Foote, K. G. 1985. Rather-high-frequency sound scattering by swimbladdered fish. Journal of the Acoustical Society of America, 78: 688–700.

Foote, K. G. 1987. Fish target strengths for use in echo-integrator surveys. Journal of the Acoustical Society of America, 82: 981–987.

Foote, K. G., and Ona, E. 1987. Tilt angles of schooling, penned saithe. Journal de Conseil International pour Exploration de la Mer, 43: 118–121.

Foote, K. G., and Traynor, J. J. 1988. Comparison of walleye pollock target-strength estimates determined from *in situ* measurements and calculations based on swimbladder form. Journal of the Acoustical Society of America, 83: 9–17.

Gorska, N., and Ona, E. 2003. Modelling the acoustic effect of swimbladder compression in herring. ICES Journal of Marine Science, 60: 548–554.

Hazen, E. L., and Horne, J. K. 2003. A method for evaluating effects of biological factors on fish target strength. ICES Journal of Marine Science, 60: 555–562.

Holliday, D. V., and Pieper, R. E. 1995. Bioacoustical oceanography at high frequencies. ICES Journal of Marine Science, 52: 279–296.

Horne, J. K. 2000. Acoustic approaches to remote species identification: a review. Fisheries Oceanography, 9(4): 356–371.

Horne, J. K. 2003. Influence of ontogeny, behaviour, and physiology on target strength of walleye pollock (*Theragra chalcogramma*). ICES Journal of Marine Science, 60: 1063–1074.

Horne, J. K., and Jech, J. M. 1999. Multi-frequency estimates of fish abundance: constraints of rather high frequencies. ICES Journal of Marine Science, 56: 184–199.

Horne, J. K., Walline, P. D., and Jech, J. M. 2000. Comparing acoustic-model predictions to *in situ* backscatter measurements of fish with dual-chambered swimbladders. Journal of Fish Biology, 57: 1105–1121.

Huse, I., and Korneliussen, R. 2000. Diel variation in acoustic-density measurements of overwintering herring (*Clupea harengus* L.). ICES Journal of Marine Science, 57: 903–910.

Huse, I., and Ona, E. 1996. Tilt-angle distribution and swimming speed of overwintering Norwegian spring spawning herring. ICES Journal of Marine Science, 53: 863–873.

Jech, J. M., Schael, D. M., and Clay, C. S. 1995. Application of three sound-scattering models to threadfin shad (*Dorosoma petenense*). Journal of the Acoustical Society of America, 98: 2262–2269.

Jørgensen, R. 2003. The effects of swimbladder size, condition and gonads on the acoustic target strength of mature capelin. ICES Journal of Marine Science, 60: 1056–1062.

Love, R. H. 1971. Measurements of fish target strength: a review. Fisheries Bulletin, 69: 703–715.

MacLennan, D. N. 1990. Acoustical measurement of fish abundance. Journal of the Acoustical Society of America, 87: 1–15.

MacLennan, D. N., Magurran, A. E., Pitcher, T. J., and Hollingworth. 1990. Behavioural determinants of fish target strength. Rapports et Procès-Verbaux des Réunions Conseil International pour l'Exploration de la Mer, 189: 245–253.

MacLennan, D. N., and Simmonds, E. J. 1992. Fisheries Acoustics. Chapman and Hall, London. 325 pp.

McClatchie, S., Alsop, J., and Coombs, R. F. 1996. A re-evaluation of relationships between fish size, acoustic frequency, and target strength. ICES Journal of Marine Science, 53: 780–791.

McClatchie, S., Macaulay, G. J., Hanchet, S. M., and Coombs, R. F. 1998. Target strength of southern blue whiting (*Micromesistius australis*) using swimbladder modelling, split beam and deconvolution. ICES Journal of Marine Science, 55: 482–493.

Midttun, L. 1984. Fish and other organisms as acoustic targets. Rapports et Procès-Verbaux des Réunions Conseil International pour l'Exploration de la Mer, 184: 25–33.

Mukai, T., and Iida, K. 1996. Depth dependence of target strength of live kokanee salmon in accordance with Boyle's law. ICES Journal of Marine Science, 53: 245–248.

Nakken, O., and Olsen, K. 1977. Target-strength measurements of fish. Rapports et Procès-Verbaux des Réunions Conseil International pour l'Exploration de la Mer, 170: 53–69.

Nøttestad, L. 1998. Extensive gas bubble release in Norwegian spring-spawning herring (*Clupea harengus*) during predator avoidance. ICES Journal of Marine Science, 55: 1133–1140.

Ona, E. 1990. Physiological factors causing natural variations in the acoustic target strength of fish. Journal of the Marine Biological Association of the United Kingdom, 70: 107–127.

Ona, E. (ed) 1999. Methodology for target-strength measurements. International Council for the Exploration of the Sea. ICES Cooperative Research Report. 235, 59.

Ona, E. 2001. Herring tilt angles measured through target tracking. Herring: Expectaions for a New Millenium 01-04, 509-519. Alaska Sea Grant.

Orlowski, A. 2001. Behavioural and physical effect of acoustic measurements of Baltic fish within a diel cycle. ICES Journal of Marine Science, 58: 1174–1183.

Sawada, K., Ye, Z., Kieser, R., McFarlane, G. A., Miyanohana, Y., and Furusawa, M. 1999. Target-strength measurements and modelling of walleye pollock and Pacific hake. Fisheries Science, 65(2): 193–205.

Thomas, G. L., Kirsch, J., and Thorne, R. E. 2002. *Ex situ* target-strength measurements of Pacific herring and Pacific sandlance. North American Journal of Fisheries Management, 22: 1136–1145.

Tytler, P., and Blaxter, J. H. S. 1973. Adaption by cod and saithe to pressure changes. Netherlands Journal of Sea Research, 7: 31–45.

Vabø, R., Olsen, K., and Huse, I. 2002. The effect of vessel avoidance of wintering Norwegian spring-spawning herring. Fisheries Research, 58: 59–77.